

# DOES A DIFFERENTIATED, CARBONATE-RICH, ROCKY OBJECT POLLUTE THE WHITE DWARF SDSS J104341.53+085558.2?

CARL MELIS<sup>1</sup> AND P. DUFOUR<sup>2</sup>

email: cmelis@ucsd.edu

<sup>1</sup>Center for Astrophysics and Space Sciences, University of California, San Diego, CA 92093-0424, USA

<sup>2</sup>Institut de Recherche sur les Exoplanètes (iREx), Université de Montréal, Montréal, QC H3C 3J7, Canada

## ABSTRACT

We present spectroscopic observations of the dust- and gas-enshrouded, polluted, single white dwarf star SDSS J104341.53+085558.2 (hereafter SDSS J1043+0855). *Hubble Space Telescope* Cosmic Origins Spectrograph far-ultraviolet spectra combined with deep Keck HIRES optical spectroscopy reveal the elements C, O, Mg, Al, Si, P, S, Ca, Fe, and Ni and enable useful limits for Sc, Ti, V, Cr, and Mn in the photosphere of SDSS J1043+0855. From this suite of elements we determine that the parent body being accreted by SDSS J1043+0855 is similar to the silicate Moon or the outer layers of Earth in that it is rocky and iron-poor. Combining this with comparison to other heavily polluted white dwarf stars, we are able to identify the material being accreted by SDSS J1043+0855 as likely to have come from the outermost layers of a differentiated object. Furthermore, we present evidence that some polluted white dwarfs (including SDSS J1043+0855) allow us to examine the structure of differentiated extrasolar rocky bodies. Enhanced levels of carbon in the body polluting SDSS J1043+0855 relative to the Earth-Moon system can be explained with a model where a significant amount of the accreted rocky minerals took the form of carbonates; specifically, through this model the accreted material could be up to 9% calcium-carbonate by mass.

*Keywords:* circumstellar matter — planet-star interactions — stars: abundances — stars: individual (SDSS J104341.53+085558.2) — white dwarfs

## 1. INTRODUCTION

Exoplanet surveys have begun to identify and characterize rocky planets with increasing frequency. As these attempts push closer to routine detection of Earth-like planets in terms of mass, radius, and orbital characteristics (e.g., [Burke et al. 2015](#)), it is natural to wonder just how Earth-like these other worlds are in terms of composition. With only masses and radii available for them, most exoplanets cannot have well-constrained compositions inferred and setting limits on their internal structure is challenging at best (e.g., [Dorn et al. 2015](#); [Rogers 2015](#); [van Lieshout et al. 2016](#), and references therein). Theoretical efforts provide some insight into how different chemical compositions in a protoplanetary disk can give rise to a range of rocky planet bulk compositions and internal structures and in some cases provide interesting comparisons to observations (e.g., [Bond et al. 2010](#); [Carter-Bond et al. 2012b,a](#); [Elser et al. 2012](#); [Moriarty et al. 2014](#); [Thiabaud et al. 2014, 2015](#); [Pignatale et al. 2016](#); [Unterborn & Panero 2016](#); [Alessi et al. 2016](#), and references therein)

While conventional exoplanet search methods are not yet able to arrive at definitive conclusions about the interior structure and bulk composition of exoplanets, studies of white dwarf stars have been providing the bulk chemical composition for rocky bodies outside of the Solar system in unprecedented detail (e.g., rare elements such as strontium and scandium — both down in abundance from hydrogen in the Sun by a factor of a billion — can be detected in the atmosphere of the most heavily polluted

white dwarfs) since the seminal publication on the topic almost a decade ago (Zuckerman *et al.* 2007). Since that time, new discoveries and capabilities have cemented the connection between disrupted rocky bodies and the pollution in the atmosphere of white dwarf stars (e.g., Vanderburg *et al.* 2015; Xu *et al.* 2016; Gänsicke *et al.* 2016; Alonso *et al.* 2016; Zhou *et al.* 2016; Rappaport *et al.* 2016, and references therein). These works – combined with the library of previous research in the field of dusty, polluted, single white dwarf stars (e.g., Debes & Sigurdsson 2002; Jura 2003, 2008; Farihi *et al.* 2009; Veras *et al.* 2016, and references therein) – show that white dwarf stars regularly accrete material from their extant planetary systems and that we can use them to characterize the composition of the accreted rocky bodies.

Enough polluted white dwarf stars are now known and sufficiently well-characterized that synthesis of these objects as a population, and the resulting insight into planets or planetesimals in the local Galaxy, can be made. Jura (2006) and Wilson *et al.* (2016) show that extrasolar planetesimals are carbon-deficient, much like the inner planetary system of our own Solar system or similar to primitive chondritic material. Jura & Xu (2012) provide insight into the prevalence of water-rich rocky bodies, showing that as a population these objects are dry,  $<1\%$  water by mass (but see Farihi *et al.* 2013; Raddi *et al.* 2015; Farihi *et al.* 2016) while Jura & Xu (2013) similarly show that refractory-rich planetesimals are unlikely to be accreted by white dwarf stars. Jura *et al.* (2013) suggest that radiogenic heating of rocky bodies through  $^{26}\text{Al}$  may be common and thus that our Solar system is not unique in having significant quantities of this nuclide. Jura *et al.* (2014) present a search methodology that can place interesting limits on evidence for plate tectonics in differentiated extrasolar rocky objects.

In this paper we present a thorough ultraviolet and optical spectroscopic inventory of the material polluting the atmosphere of the dust- and gas-disk hosting single white dwarf star SDSS J104341.53+085558.2 (hereafter SDSS J1043+0855). We find this material to be rocky in general, extremely depleted in iron, and enhanced in carbon relative to rocky material in the inner parts of our Solar system. A synthesis of all heavily polluted white dwarf star measurements is made, resulting in a strong suggestion that some white dwarfs are experiencing pollution from specific regions of differentiated rocky bodies, thus opening a window into extrasolar rocky body structure. Carbonates are proposed as a possible carrier of the enhanced carbon signature for the parent body polluting SDSS J1043+0855 and the implications of such a scenario are discussed.

## 2. OBSERVATIONS

### 2.1. Ultraviolet Spectroscopy

*Hubble Space Telescope* Cosmic Origins Spectrograph (hereafter COS; Green *et al.* 2012) observations were obtained for SDSS J1043+0855 on 2015 April 27. Two spacecraft orbits were awarded to this target as part of GO program 13700 and we obtained a total exposure time of 5105 seconds with the G130M grating centered at a wavelength of 1291 Å. Observations were obtained in the TIME-TAG mode using the 2.5" diameter primary science aperture. Four different FP-POS values were utilized during the observations (about a quarter of the total time was spent in each) to minimize fixed pattern noise in the detector. This setup yields spectral resolving power of  $\approx 20,000$  and final spectral coverage from 1133 to 1433 Å except for a gap from 1279 to 1288 Å.

The raw COS data were processed with the CALCOS pipeline 3.0, coadded with the use of the IDL script COADD\_X1D (Danforth *et al.* 2010; Keeney *et al.* 2012), and then smoothed with a boxcar of six pixels. The resulting signal-to-noise-ratio (S/N) per pixel in the smoothed data is  $\approx 14$  at a wavelength of 1320 Å. The final spectrum presented here is flux calibrated and in vacuum wavelengths corrected to the heliocentric reference frame. Following Jura *et al.* (2012), we use the `timefilter` module to extract the night-time portion of the data around the O I lines between 1300 and 1308 Å to help mitigate terrestrial day airglow emission. This is mostly done as a sanity check on the abundance for the one

uncontaminated O I line near 1152 Å which otherwise would be the only line to inform the oxygen abundance in SDSS J1043+0855. Lower S/N spectra are obtained for the O I lines between 1300 and 1308 Å as a result of the filtering and abundances consistent with the 1152 Å line are obtained.

## 2.2. Optical Spectroscopy

Melis *et al.* (2010) provide a detailed accounting of Keck HIRES (Vogt *et al.* 1994) optical echelle spectra that were obtained for SDSS J1043+0855. Optical observations obtained by Melis *et al.* (2010) had an aim of exploring the gaseous component of the debris disk orbiting the white dwarf star. In this work we re-reduce the HIRES data with a focus on making measurements or obtaining tight limits for metal absorption lines in the spectra. Data were reduced using the MAKEE software package which outputs heliocentric velocity corrected spectra shifted to vacuum wavelengths. After reduction and extraction, high order polynomials are fit to each order to bring overlapping order segments into agreement before combining all orders of every HIRES exposure to generate a final spectrum for analysis.

## 3. RESULTS AND MODELING

We adopt SDSS J1043+0855 stellar parameters from Tremblay *et al.* (2011): a DA white dwarf with effective temperature of 18,330 K,  $\log g$  of 8.05 (cgs), resulting mass of  $0.626 M_{\odot}$ , and a “thin envelope” having mass ratio  $q = M_{\text{env}}/M_{\text{WD}} = 10^{-16.645}$ . We note that these parameters are, to within quoted errors in each source paper, consistent with those given by Manser *et al.* (2016). With these parameters we proceed in fitting the metallic absorption lines detected in the COS and HIRES spectra and deriving upper limits for elements of interest. Fitting proceeds very similar as to the description given in Melis *et al.* (2011) and references therein. We use a local thermodynamic equilibrium (LTE) model atmosphere code similar to that described in Dufour *et al.* (2005, 2007) and absorption line data are taken from the Vienna Atomic Line Database.

We calculate grids of synthetic spectra for each element of interest covering a range of abundances typically from  $\log[n(\text{Z})/n(\text{H})] = -3.0$  to  $-8.0$  in steps of 0.5 dex. We then determine the abundance of each element by fitting the various observed lines using a similar method to that described in Dufour *et al.* (2005). Briefly, this is done by minimizing the value of  $\chi^2$  taken as the sum over all frequencies of the difference between the normalized observed and model fluxes (the synthetic spectra are multiplied by a constant factor to account for the solid angle and the slope of the spectra locally are allowed to vary by a first order polynomial to account for residuals from the normalization procedure), all frequency points being given an equal weight. Interpolation between grid points allows us to achieve individual line abundances accurate to  $<0.05$  dex. This is done individually for each line and the final adopted abundances (see Table 1) are taken to be the average of all the measurements made for a given element. Uncertainties were taken to be the dispersion among abundance values used in the average. If this dispersion was less than 0.20 dex, then the abundance uncertainty is set to 0.20 dex. For elements where only one line is available to derive the abundance, the uncertainty is set to 0.30 dex. It is noted that changing the effective temperature by  $\pm 500$  K and/or the surface gravity by  $\pm 0.1$  dex (typical of uncertainties for white dwarf stellar atmospheric modeling) changes derived abundances by less than 0.1 dex, indicating that the relative abundance ratios are not sensitive to the exact final stellar parameters adopted.

We find contributions from C, O, Al, Si, P, S, Fe, and Ni in the COS data and Ca, Mg, and Si in the HIRES data (Figure 1). Additionally, we derive from COS data restrictive upper limits for Sc, Ti, V, Cr, and Mn (see Table 1) and from HIRES data a non-restrictive upper limit for  $\log[n(\text{Na})/n(\text{H})]$  of  $<10^{-5}$  (this value is not quoted in the table). Abundances for all elements identified in the atmosphere of SDSS J1043+0855 are reported in Table 1 as well as upper limits for other elements of interest (see Section 4). S is a tentative detection and the suggested abundance can be taken as a firm upper limit; higher S/N data can better reveal this element. We note that, similar to Gänsicke *et al.* (2012)

and references therein, we find a discrepancy between the abundance for Si as derived from optical and ultraviolet data (see discussion in [Gänsicke et al. 2012](#) for reasons why these values may not agree). We adopt here the average of the optical and ultraviolet Si abundances and set the error to cover the difference between them (Table 1).

Interstellar lines are present in the optical and ultraviolet spectra, particularly near the ultraviolet C lines. For C, these lines are readily identifiable by their reversed line strength ratio due to the material being in a dramatically different physical environment than the atmosphere of the white dwarf star. All interstellar lines are also offset in radial velocity relative to the stellar photospheric velocity. [Melis et al. \(2010\)](#) measure a photospheric velocity (which includes gravitational redshift) of  $+39 \pm 4 \text{ km s}^{-1}$ , a value reproduced within the uncertainties by all new photospheric elements presented herein. Interstellar lines, specifically C and Ca, have velocity near  $0 \text{ km s}^{-1}$  (see also [Melis et al. 2010](#)). We note the excellent agreement of optical abundance values for Ca, Mg, and Si with those reported in [Manser et al. \(2016\)](#).

#### 4. DISCUSSION

Previous work has shown that SDSS J1043+0855 is host to both gaseous and dusty debris within its tidal radius ([Gänsicke et al. 2007](#); [Melis et al. 2010](#); [Brinkworth et al. 2012](#); [Manser et al. 2016](#)), suggesting that any metal pollution seen in its atmosphere originated in the tidal disruption and subsequent accretion of a rocky object from the white dwarf’s extant planetary system (e.g., [Jura 2003](#)). Following this line of logic, we can estimate the elemental composition of the material currently being accreted by examining the metal abundances reported in Table 1. Similar to the case of the hot white dwarf GALEX J193156.8+011745 as described in [Melis et al. \(2011\)](#), we expect that SDSS J1043+0855 is in the steady-state accretion phase and that radiative levitation is negligible (see also [Xu et al. 2013, 2014](#)). We then use Equation 16 from [Jura et al. \(2009\)](#) and diffusion constants calculated by G. Fontaine<sup>1</sup> (private comm., 2016; see Table 1 and [Dufour et al. 2016](#)) with the parameters for SDSS J1043+0855 to estimate the accretion rate and abundance ratio relative to Mg of the polluting material for each element (Si is not used for this comparison because of the high adopted uncertainty for its abundance – see Section 3).

Accreted abundances by number relative to Mg and mass accretion rates are reported in Table 1. Distinct amongst these are high levels of carbon ( $\approx 1\%$  by mass) and calcium ( $\approx 7\%$  by mass) and deficient iron ( $\approx 10\%$  by mass). The significant deficit of iron is reminiscent of the abundances for the surface of the Moon (hereafter the silicate Moon) or for the crust and mantle of the Earth (compare with Figure 7 of [Jura & Young 2014](#)). To help illustrate this, Table 1 also reports metal abundance ratios relative to magnesium for the silicate Moon as taken from Table 4.7 of [Lodders & Fegley \(2011\)](#) with the exception of carbon which comes from [Wetzel et al. \(2015\)](#). Comparison between the silicate Moon and measurements for SDSS J1043+0855 are also plotted in Figure 2. Also displayed in Figure 2 is a “Hollow Earth” model. This model is constructed in a similar fashion as the “wind-stripped Earth” model presented in Figure 6 of [Melis et al. \(2011\)](#), except it starts removing material from the core and works its way out toward the crust. We remove varying fractions of the core, then lower mantle, then upper mantle and compute the resulting bulk abundances of the remaining material relative to magnesium. The best match with the data for SDSS J1043+0855 is shown in Figure 2 and corresponds to removing the entire core and lower mantle of the Earth (this is similar to the case of NLTT 43806; see [Zuckerman et al. 2011](#) and discussion below).

Based on the comparison shown in Figure 2 it would seem plausible that SDSS J1043+0855 is accreting the surface layers of either an exomoon (e.g., [Payne et al. 2016](#)) or fully-differentiated massive rocky body. The agreement between enhancements in nickel and calcium relative to the silicate Moon

<sup>1</sup> <http://dev.montrealwhitedwarfdatabase.org/evolution.html>



for both the Hollow Earth model and SDSS J1043+0855 possibly suggest better agreement with the latter scenario, although this relies on strong assumptions about commonality between the parent body feeding SDSS J1043+0855 and the Earth (an assumption clearly not borne out by elements like aluminum and carbon); a way to further test this idea would be through tighter limits on manganese, chromium, and especially titanium (which is strongly depleted for the surface layers of the Earth).

Corroboration of a massive differentiated body as an appropriate interpretation could come from limits on the total mass of the accreted body. However, from the total mass accretion rate of  $\approx 1.3 \times 10^8 \text{ g s}^{-1}$  and under the assumption of this being constant over a disk lifetime of  $\sim 1 \text{ Myr}$  (Melis *et al.* 2011; Girven *et al.* 2012), we arrive at an estimate for the total initial mass of the rocky material of  $\sim 4 \times 10^{21} \text{ g}$ . This is well below the estimated total mass of any planet or major moon in the Solar system. But, as discussed earlier in this section and as outlined in detail below, the body being accreted by SDSS J1043+0855 very likely was differentiated and as such should have been at least as massive as objects like Vesta or Ceres in our Solar system ( $10^{23}$ - $10^{24} \text{ g}$ ; as far as we know, these are the least massive differentiated bodies in the Solar system). As such, we should view the total mass given above as a lower limit; indeed, the assumption that the currently observed accretion rate would be constant over the entire disk lifetime is suspect as several studies find instead evidence that greatly enhanced accretion rates can be realized during the evolution of a white dwarf debris disk (e.g., Rafikov 2011a,b; Girven *et al.* 2012; Farihi *et al.* 2012; Wyatt *et al.* 2014). Alternatively, and as described in more detail below, it could be the case that only a small fraction of rocky material was liberated from a differentiated parent body and subsequently delivered to SDSS J1043+0855 (see also Zuckerman *et al.* 2011).

Simulation work suggests that it is unlikely that a full-fledged planet (Mars-like or more massive) would be delivered to the tidal destruction radius of a white dwarf star (e.g., Debes & Sigurdsson 2002; Jura 2008; Mustill *et al.* 2014; Veras & Gänsicke 2015; Veras *et al.* 2016). As discussed by Zuckerman *et al.* (2011), it is not necessary to deliver an entire planet-sized object into the tidal destruction radius of a polluted white dwarf star, even when there is evidence for the material to have come from particular layers of a differentiated rocky body. One need only to liberate some amount of material from the relevant region that is believed to now be polluting the white dwarf star under study. Having just some pieces removed from a differentiated rocky body – especially surface material – is rather plausible as evidenced by simulations of giant impact type collisions during rocky planet formation (e.g., Asphaug 2014 and references therein; Melis *et al.* 2011 describes how deeper layers may become more readily exposed before impact liberation occurs). Indeed, such collisions could very well generate material with an orbit that would take it to where it would be gravitationally captured and eventually accreted by the host white dwarf star. The situation with moons that are much smaller than Mars could be somewhat different as it is probably possible to get such objects in whole into their host white dwarf’s tidal destruction radius (e.g., Payne *et al.* 2016).

Perhaps most striking in Figure 2 is the dramatic enhancement of carbon in the parent body being accreted by SDSS J1043+0855 relative to the silicate Moon and the “Hollow Earth” model. It is worth noting that measurements of carbon in the Moon and for the surface layers of the Earth have produced a wide range of results in the past with values as much as two orders of magnitude larger than that reported in Table 1. We use the value from Wetzel *et al.* (2015) who have made significant improvements over previous attempts. As such, while their measurement is the state-of-the-art, it bears mentioning that measurements of carbon for the Moon and surface layers of Earth have a shaky past. Regardless, the enhancement of carbon in the body polluting SDSS J1043+0855 relative to the surface of the Earth and the Moon will likely remain (even if at some lower level).

White dwarfs that are accreting rocky material  $\gtrsim 1\%$  carbon by mass have been previously reported (e.g., Xu *et al.* 2013; Jura *et al.* 2015; Wilson *et al.* 2015, 2016), although each of these are helium-dominated atmosphere white dwarfs while SDSS J1043+0855 is hydrogen-dominated. The

importance of this distinction is discussed in [Wilson \*et al.\* \(2015\)](#) and summarized here: helium-atmosphere white dwarfs are susceptible to dredge-up from the interior of the white dwarf star which can implant sufficient carbon to explain observations to date. A hydrogen-atmosphere white dwarf, especially at the temperature of SDSS J1043+0855, would not have atmospheric carbon pollution as a result of such a mechanism. SDSS J1043+0855 could thus be considered the first high-carbon content polluted white dwarf where the carbon is unambiguously delivered by outside sources. However, with this designation comes the inevitable conclusion that other such white dwarfs are probably similar.

Something that is thus far unique to the case of SDSS J1043+0855 is the C/O ratio realized for its polluting material. While carbon does not dominate over oxygen, the C/O ratio does lie squarely in between the “bi-modal” distribution suggested for bodies polluting white dwarf stars in [Wilson \*et al.\* \(2016\)](#). This suggests that there is indeed more diversity within exoplanetary rocky bodies yet to be discovered and that distinctly non-Solar system-like material does seem to exist in the local Galaxy, although it does appear to be rare. It is desirable to know how the carbon was originally delivered to the rocky body that is now being accreted by SDSS J1043+0855 and how it populated the rocky body such that it remained entrained through to the white dwarf phase of stellar evolution. Below we explore a plausible idea for the retainment of the carbon that is thus far consistent with the data available.

Following [Klein \*et al.\* \(2010, 2011\)](#) and [Farihi \*et al.\* \(2013\)](#), we attempt to balance the accreted oxygen abundance under the expectation that all oxygen was contained in rocky oxygenated minerals (e.g., MgO, Al<sub>2</sub>O<sub>3</sub>, SiO<sub>2</sub>, CaO, FeO, and NiO). In this way, we find that – within the errors – oxygen is roughly critically distributed into rocky minerals (a small oxygen excess results from inclusion of just the above mentioned metal oxides). Some forms of carbon (e.g., CO<sub>2</sub>) might be lost in a manner similar to water during the host star’s asymptotic giant branch phase of evolution (see [Jura & Xu 2010](#)). Suppose that the carbon in the parent body now being accreted by SDSS J1043+0855 was instead locked up in carbonate minerals and as such would be less susceptible to loss mechanisms. Of the elements seen thus far in spectroscopic observations of SDSS J1043+0855, we could construct the following naturally occurring carbonates (on Earth): CaCO<sub>3</sub>, MgCO<sub>3</sub>, and FeCO<sub>3</sub>. CaCO<sub>3</sub> in particular has already been seen in various space environments (e.g., [Kemper \*et al.\* 2002b](#); [Kemper \*et al.\* 2002a](#); [Chiavassa \*et al.\* 2005](#); [Boynton \*et al.\* 2009](#); [de Sanctis \*et al.\* 2016](#)), and thus is a reasonable candidate for also being present in the material being accreted by SDSS J1043+0855.

We examine two possibilities: (i) a generic carbonate scenario where we just account for how much CO<sub>2</sub> would be necessary and what the impact would be on the oxygen budget, and (ii) a scenario where all carbon is locked up in CaCO<sub>3</sub>. Both scenarios will have a similar impact on the oxygen budget, but in the second scenario we can make an estimate for what the maximum fraction by mass the parent body could have been in calcium-carbonate. We find in general that allowing carbonates in the oxygen budget calculation results in a  $\approx 3\%$  overtaking of the available oxygen (note that it is assumed that all Fe is in the form of FeO which maximizes its contribution to the oxygen budget). If no carbonates are allowed in the oxygen budget calculation, then an oxygen excess of  $\approx 5\%$  is instead obtained. The maximum mass fraction of CO<sub>2</sub> that can be realized in scenario (i) is  $\approx 4\%$ . In scenario (ii), the maximum mass fraction of CaCO<sub>3</sub> that can be realized is  $\approx 9\%$ . The result of the oxygen balance analysis is that it appears as though the material being accreted by SDSS J1043+0855 very likely originated in rocky minerals, is only a small percentage (if any) of water by mass (see e.g., [Farihi \*et al.\* 2013](#)), and could host a significant quantity of carbonates – especially calcium-carbonate – by mass.

It is noted that cometary bodies in the Solar system are known to contain  $\approx 5\%$  CO<sub>2</sub> by mass (e.g., [Jessberger \*et al.\* 1989](#)), very similar to the scenario outlined above for the carbon and oxygen excess in the accreted material polluting SDSS J1043+0855. However, a cometary origin for the material polluting this white dwarf star is not very likely for at least the following reasons: (i) comets can be

up to 80% water by mass, whereas the object being accreted by SDSS J1043+0855 is at best equal parts water and CO<sub>2</sub> by mass. Having a comet that somehow loses all its water but none of its CO<sub>2</sub> is improbable, especially if one considers the loss mechanisms outlined in [Jura & Xu \(2010\)](#). (ii) The otherwise good agreement of the abundances measured in the atmosphere of SDSS J1043+0855 with Earth’s crust would be hard to reconcile given that comets appear rather primitive in their rocky elements (e.g., [Jessberger et al. 1989](#)). Thus, we reject extrasolar comet-like bodies as a viable candidate for explaining the material polluting SDSS J1043+0855.

White dwarfs that are iron-poor or that otherwise have Earth surface-layer-like compositions have been previously reported (e.g., [Zuckerman et al. 2011](#); [Farihi et al. 2013](#); [Raddi et al. 2015](#)). Having securely identified four examples of such systems now with the characterization of SDSS J1043+0855, it seems prudent to evaluate how such systems compare to other well-characterized polluted white dwarfs. We do this by collecting relative abundances and mass fractions of accreted elements for all available white dwarf stars. We only consider those objects where each of iron, magnesium, silicon, and oxygen have been measured. There are a few exceptions: GD 362 where limits on oxygen are sufficiently deep to robustly estimate its contribution to the total mass of the accreted body (e.g., [Xu et al. 2013](#)), and PG 1225–079 and NLTT 43806 where estimates of the oxygen mass fraction are made assuming all metals – excluding and including iron, respectively – originate in metal oxides (see below).

Examining this collection reveals a trend in accreted abundance ratios for Si/Fe vs Mg/Fe that is suggestive of whether accreted material originates from the inner or outer regions of a rocky body (Figure 3). Fe-poor objects in the “Crust-like” area of Figure 3 are strongly suggestive of having an origin in the outer-most layers of a differentiated rocky body. The majority of the Fe in these objects got locked up deep in their interiors as a result of the differentiation process and only the surface crust and mantle material was delivered to the host white dwarf. Fe-rich objects in the “Core-like” area of the figure instead resemble objects whose outer-most layers were removed and only the inner parts were delivered to the white dwarf (e.g., [Melis et al. 2011](#)). Verification that these bodies truly are iron-poor or iron-rich as suggested by their placement in the “Crust-like” or “Core-like” regions of Figure 3 comes from calculating the mass fraction of iron in the parent body material being accreted in each white dwarf system (bottom panel of Figure 3).

This overall trend in heavily polluted white dwarf stars provides not only clues as to what the evolutionary history of accreted material is, but also strongly suggests that white dwarf stars can be used to examine the chemical composition of *specific regions* of an extrasolar rocky body in specialized cases. An exciting prospect of this interpretation is its potential to inform us on the diversity of the crust-mantle regions (i.e., surfaces) of alien worlds and its implications for the prevalence of water-rich – vastly more so than the Earth – differentiated rocky objects. NLTT 43806, one of the four systems found in the “Crust-like” area of Figure 3, is distinctly Earth-like in its high mass fraction of aluminum ([Zuckerman et al. 2011](#)). It is worth noting that all other “Crust-like” white dwarfs fall below the Al/Mg ratio of the silicate Moon similar to SDSS J1043+0855 in Figure 2; whether this apparent bi-modality in Al-content of “Crust-like” white dwarfs continues to manifest as more objects are discovered and characterized will be interesting as Al is thought to be tied to melt processes in the surface of the Earth (J. Day, private comm. 2016). GD 61 and SDSS J1242+5226, the two remaining “Crust-like” objects, accrete rocky bodies which both show evidence for significant water pollution.

Recognizing that the outer layers of the Earth amount to only about 10% of the total mass of the planet and given the total mass estimates for the parent bodies polluting “Crust-like” white dwarfs, it is plausible to interpret material polluting these white dwarf stars as having its origin in the surface layers of a full-fledged planet (see also discussion in [Zuckerman et al. 2011](#)). If correct, this interpretation would suggest that out of four examples of “Crust-like” rocky material sampled to date, one is distinctly Earth-like, two are extremely water-rich, and one shows enhanced carbon

that could plausibly have had its origin in carbonates. While clearly within the realm of statistics of small numbers, these possibilities surely warrant deeper investigation and a broader search for similarly iron-poor polluted white dwarf stars.

It is of some value to consider the implications of SDSS J1043+0855 as being polluted by the outer layers of a massive, differentiated rocky body rich in carbonates, specifically calcium-carbonate. In general, carbonates on Earth and other space environments (including, but not limited to: Ceres, Mars, protoplanetary disks, evolved stars, and planetary nebulae; see [de Sanctis et al. 2016](#), [Boynton et al. 2009](#), [Chiavassa et al. 2005](#), [Kemper et al. 2002a](#), [Kemper et al. 2002b](#), respectively) typically require some amount of water to form (e.g., [Toppani et al. 2005](#)). To produce on the order of several percent of the mass of an object’s surface in carbonates would thus suggest a reasonable liquid water reservoir coupled with some effective CO<sub>2</sub>-delivery mechanism (whether that would be in the form of a dense atmosphere, intense outgassing, or some other mechanism), similar to the conditions that could have led to the generation of calcium-carbonate in other space environments ([Toppani et al. 2005](#)). This argues for the possibility of a liquid water ocean in the outer layers of the parent body now being accreted by SDSS J1043+0855. If true, either this water was removed during the star’s post-main sequence evolution (e.g., [Jura & Xu 2010](#)) or is sufficiently small in mass fraction to be undetectable within our current measurement capabilities (note that our ocean is  $\approx 0.02\%$  of Earth’s mass).

Calcium-carbonate on the Earth is typically associated with marine organisms which utilize it as a part of their exoskeletal structures. As mentioned above, calcium-carbonate can be seen in a variety of space environments and so it is of course possible to generate the mineral through non-biological pathways (but see also the discussion regarding entraining CO<sub>2</sub> through the aid of life by [Haqq-Misra et al. 2016](#)). Perhaps more vexing for having this mineral originate through life processes is the extremely short main sequence lifetime of the progenitor star of SDSS J1043+0855 (with a mass of  $2.76 \pm 0.04 M_{\odot}$  as given by [Manser et al. 2016](#), this star would have evolved off of the main sequence in  $\lesssim 1$  Gyr).

Calcium-carbonate in the surface of the world now being accreted by SDSS J1043+0855 could have been synthesized rapidly as the mineral travertine through plate tectonic processes that release CO<sub>2</sub> and geothermal energy in an aqueous environment. Some evidence in favor of such an interpretation already exists. Recall that the pollution for all four of the “Crust-like” white dwarfs has distinctly oceanic crust-like signatures of Mg/Fe (Figure 3). The oceanic crust in Earth is regularly polluted by upwellings of magnesium-rich material from the mantle through subduction and recycling (plate tectonics processes). This results in Fe being depleted relative to Mg in addition to it being depleted relative to Si as one would expect in the Si-dominated continental crust of Earth. Mg and Si in the oceanic crust are comparable and substantially more abundant than Fe, while in the continental crust Fe and Mg have comparable abundance and are both strongly depleted relative to Si (see Figure 3). Additionally, the strong evidence for water in at least two of the “Crust-like” polluted white dwarfs (and circumstantial evidence for water in all of them) suggests atmospheric conditions that allow water to persist through the object’s life, a characteristic considered prerequisite for tectonic activity (consider the comparison between dry Venus which has no plate tectonics and the Earth; e.g., [Kaula & Phillips 1981](#); [Barnes et al. 2009](#)). If this hypothesis pans out, then the results herein would represent the first evidence for plate tectonics outside of the Solar system (e.g., see [Jura et al. 2014](#)).

While it is fun to speculate about the origin of any carbonates in this object, what can be done to confirm that such minerals are actually present? The launch of the *James Webb Space Telescope* is imminent, and with it will return a capability to perform sensitive mid-infrared spectroscopic observations ([Rieke et al. 2015](#); [Kendrew et al. 2015](#)). Mid-infrared spectroscopy of SDSS J1043+0855 could detect a characteristic signature of CaCO<sub>3</sub> in the disk that orbits it (e.g., [Kemper et al. 2002a](#)),



thus validating some of the speculative discussion given here. In the meantime, coupled dynamical and chemical evolution-tracking simulations (such as those in [Bond \*et al.\* 2010](#)) can explore how one might obtain a rocky body with the chemical abundances exhibited by that being accreted by SDSS J1043+0855.

## 5. CONCLUSIONS

Spectroscopic observations of SDSS J1043+0855 in the ultraviolet and optical reveal a suite of elements that suggest a parent body that is rocky and iron-poor. Synthesizing all available heavily-polluted white dwarf measurements, we find a trend in the accreted abundance ratios for Si/Fe vs Mg/Fe suggestive of whether accreted material could have originated from the inner or outer regions of a differentiated object; we use this trend to identify the material polluting SDSS J1043+0855 as having its origin in the outer layers of a differentiated, massive, rocky body. Enhanced levels of carbon can be explained by a model where the rocky body polluting SDSS J1043+0855 hosted significant quantities of carbonate minerals – this combined with a mild enhancement of calcium suggests the possibility of calcium-carbonate. Future observations with *JWST* can explore this interpretation while modeling can provide insight into the formation mechanisms and evolutionary paths such material might have experienced leading up to its subsequent tidal destruction and accretion by SDSS J1043+0855.

C.M. would like to acknowledge the profound impact the late Prof. Michael Jura had on his development into a scientist; he will be sorely missed, especially within the community who study white dwarf planetary systems. Indeed, the present paper benefited significantly from discussions with Prof. Jura. We would like to thank Prof. Ben Zuckerman for useful discussion and comments on multiple versions of the text presented here. We thank Prof. James Day for useful insight regarding aluminum and Prof. Steve Desch for suggesting travertine and plate tectonics as a possibility. We thank the anonymous referee for suggestions that helped improve this paper. C.M. was supported by grants from the National Science Foundation (AST-1313428) and NASA (NNX14AF76G and HST-GO-13700.001-A). P.D. acknowledges support in part by the NSERC Canada and by the Fund FRQNT (Québec). This paper is based on observations made with the NASA/ESA *Hubble Space Telescope*, obtained at the Space Telescope Science Institute, which is operated by the Association of Universities for Research in Astronomy, Inc., under NASA contract NAS 5-26555. Some of the data presented herein were obtained at the W.M. Keck Observatory, which is operated as a scientific partnership among the California Institute of Technology, the University of California and the National Aeronautics and Space Administration. The Observatory was made possible by the generous financial support of the W.M. Keck Foundation. The authors wish to recognize and acknowledge the very significant cultural role and reverence that the summit of Mauna Kea has always had within the indigenous Hawaiian community. We are most fortunate to have the opportunity to conduct observations from this mountain. This research has made use of NASA’s Astrophysics Data System.

*Facilities:* HST (COS), Keck:I (HIRES)

*Software:* MAKEE, IRAF, IDL

## REFERENCES

- |   |  |
|---|--|
| <p>Alessi, M., Pudritz, R. E., &amp; Cridland, A. J. 2016, <i>ArXiv e-prints</i></p> <p>Allègre, C. J., Poirier, J., Humler, E., &amp; Hofmann, A. W. 1995, <i>Earth and Planetary Science Letters</i>, <b>134</b>, 515</p> <p>Alonso, R., Rappaport, S., Deeg, H. J., &amp; Palte, E. 2016, <i>A&amp;A</i>, <b>589</b>, L6</p> | <p>Anderson, D. L. 1989, <i>Theory of the Earth</i>. Blackwell Scientific Publications (Oxford, UK)</p> <p>Asphaug, E. 2014, <i>Annual Review of Earth and Planetary Sciences</i>, <b>42</b>, 551</p> <p>Barnes, R., Jackson, B., Greenberg, R., &amp; Raymond, S. N. 2009, <i>ApJL</i>, <b>700</b>, L30</p> |
|---|--|

- Bond, J. C., O'Brien, D. P., & Lauretta, D. S. 2010, *ApJ*, **715**, 1050
- Boynton, W. V., *et al.* 2009, *Science*, **325**, 61
- Brinkworth, C., Gaensicke, B., Girven, J., Hoard, D., Marsh, T., Parsons, S., & Koester, D. 2012, *ArXiv e-prints*
- Burke, C. J., *et al.* 2015, *ApJ*, **809**, 8
- Carter-Bond, J. C., O'Brien, D. P., Delgado Mena, E., Israelian, G., Santos, N. C., & González Hernández, J. I. 2012a, *ApJL*, **747**, L2
- Carter-Bond, J. C., O'Brien, D. P., & Raymond, S. N. 2012b, *ApJ*, **760**, 44
- Chiavassa, A., Ceccarelli, C., Tielens, A. G. G. M., Caux, E., & Maret, S. 2005, *A&A*, **432**, 547
- Danforth, C. W., Keeney, B. A., Stocke, J. T., Shull, J. M., & Yao, Y. 2010, *ApJ*, **720**, 976
- de Sanctis, M. C., *et al.* 2016, *Nature*, **536**, 54
- Debes, J. H. & Sigurdsson, S. 2002, *ApJ*, **572**, 556
- Dorn, C., Khan, A., Heng, K., Connolly, J. A. D., Alibert, Y., Benz, W., & Tackley, P. 2015, *A&A*, **577**, A83
- Dufour, P., Bergeron, P., & Fontaine, G. 2005, *ApJ*, **627**, 404
- Dufour, P., Kilic, M., Fontaine, G., Bergeron, P., Lachapelle, F., Kleinman, S. J., & Leggett, S. K. 2010, *ApJ*, **719**, 803
- Dufour, P., Kilic, M., Fontaine, G., Bergeron, P., Melis, C., & Bochanski, J. 2012, *ArXiv e-prints*
- Dufour, P., Blouin, S., Coutu, S., Fortin-Archambault, M., Thibeault, C., Bergeron, P., & Fontaine, G. 2016, *ArXiv e-prints*
- Dufour, P., *et al.* 2007, *ApJ*, **663**, 1291
- Elser, S., Meyer, M. R., & Moore, B. 2012, *Icarus*, **221**, 859
- Farihi, J., Gänsicke, B. T., & Koester, D. 2013, *Science*, **342**, 218
- Farihi, J., Gänsicke, B. T., Wyatt, M. C., Girven, J., Pringle, J. E., & King, A. R. 2012, *MNRAS*, **424**, 464
- Farihi, J., Jura, M., & Zuckerman, B. 2009, *ApJ*, **694**, 805
- Farihi, J., *et al.* 2016, *MNRAS*
- Gänsicke, B. T., Koester, D., Farihi, J., Girven, J., Parsons, S. G., & Breedt, E. 2012, *MNRAS*, **424**, 333
- Gänsicke, B. T., Marsh, T. R., & Southworth, J. 2007, *MNRAS*, **380**, L35
- Gänsicke, B. T., *et al.* 2016, *ApJL*, **818**, L7
- Girven, J., Brinkworth, C. S., Farihi, J., Gänsicke, B. T., Hoard, D. W., Marsh, T. R., & Koester, D. 2012, *ArXiv e-prints*
- Green, J. C., *et al.* 2012, *ApJ*, **744**, 60
- Haqq-Misra, J., Kopparapu, R. K., Batalha, N. E., Harman, C. E., & Kasting, J. F. 2016, *ArXiv e-prints*
- Jessberger, E. K., Kissel, J., & Rahe, J., 1989 *The composition of comets*, 167–191
- Jura, M. 2003, *ApJL*, **584**, L91
- 2006, *ApJ*, **653**, 613
- 2008, *AJ*, **135**, 1785
- Jura, M., Dufour, P., Xu, S., Zuckerman, B., Klein, B., Young, E. D., & Melis, C. 2015, *ApJ*, **799**, 109
- Jura, M., Klein, B., Xu, S., & Young, E. D. 2014, *ApJL*, **791**, L29
- Jura, M., Muno, M. P., Farihi, J., & Zuckerman, B. 2009, *ApJ*, **699**, 1473
- Jura, M. & Xu, S. 2010, *AJ*, **140**, 1129
- 2012, *AJ*, **143**, 6
- 2013, *AJ*, **145**, 30
- Jura, M., Xu, S., Klein, B., Koester, D., & Zuckerman, B. 2012, *ApJ*, **750**, 69
- Jura, M., Xu, S., & Young, E. D. 2013, *ApJL*, **775**, L41
- Jura, M. & Young, E. D. 2014, *Annual Review of Earth and Planetary Sciences*, **42**, 45
- Kaula, W. M. & Phillips, R. J. 1981, *Geophys. Res. Lett.*, **8**, 1187
- Keeney, B. A., Danforth, C. W., Stocke, J. T., France, K., & Green, J. C. 2012, *PASP*, **124**, 830
- Kemper, F., Molster, F. J., Jäger, C., & Waters, L. B. F. M. 2002a, *A&A*, **394**, 679
- Kemper, F., *et al.* 2002b, *Nature*, **415**, 295
- Kendrew, S., *et al.* 2015, *PASP*, **127**, 623
- Klein, B., Jura, M., Koester, D., & Zuckerman, B. 2011, *ApJ*, **741**, 64
- Klein, B., Jura, M., Koester, D., Zuckerman, B., & Melis, C. 2010, *ApJ*, **709**, 950
- Koester, D. 2009, *A&A*, **498**, 517
- Lodders, K & Fegley, B. 2011, *Chemistry of the Solar System*. RSC Publishing (Cambridge, UK)
- Manser, C. J., Gaensicke, B. T., Koester, D., Marsh, T. R., & Southworth, J. 2016, *ArXiv e-prints*
- Melis, C., Jura, M., Albert, L., Klein, B., & Zuckerman, B. 2010, *ApJ*, **722**, 1078
- Melis, C., *et al.* 2011, *ApJ*, **732**, 90
- Moriarty, J., Madhusudhan, N., & Fischer, D. 2014, *ApJ*, **787**, 81
- Mustill, A. J., Veras, D., & Villaver, E. 2014, *MNRAS*, **437**, 1404
- Payne, M. J., Veras, D., Holman, M. J., & Gänsicke, B. T. 2016, *MNRAS*, **457**, 217
- Pignatale, F. C., Liffman, K., Maddison, S. T., & Brooks, G. 2016, *MNRAS*, **457**, 1359
- Raddi, R., *et al.* 2015, *MNRAS*, **450**, 2083
- Rafikov, R. R. 2011a, *ApJL*, **732**, L3
- 2011b, *MNRAS*, **416**, L55
- Rappaport, S., Gary, B. L., Kaye, T., Vanderburg, A., Croll, B., Benni, P., & Foote, J. 2016, *MNRAS*, **458**, 3904
- Rieke, G. H., *et al.* 2015, *PASP*, **127**, 584
- Rogers, L. A. 2015, *ApJ*, **801**, 41
- Thiabaud, A., Marboeuf, U., Alibert, Y., Cabral, N., Leya, I., & Mezger, K. 2014, *A&A*, **562**, A27
- Thiabaud, A., Marboeuf, U., Alibert, Y., Leya, I., & Mezger, K. 2015, *A&A*, **580**, A30
- Toppani, A., Robert, F., Libourel, G., de Donato, P., Barres, O., D'Hendecourt, L., & Ghanbaja, J. 2005, *Nature*, **437**, 1121
- Tremblay, P.-E., Bergeron, P., & Gianninas, A. 2011, *ApJ*, **730**, 128
- Unterborn, C. T. & Panero, W. R. 2016, *ArXiv e-prints*
- van Lieshout, R., *et al.* 2016, *ArXiv e-prints*
- Vanderburg, A., *et al.* 2015, *Nature*, **526**, 546
- Veras, D. & Gänsicke, B. T. 2015, *MNRAS*, **447**, 1049
- Veras, D., Mustill, A. J., Gänsicke, B. T., Redfield, S., Georgakarakos, N., Bowler, A. B., & Lloyd, M. J. S. 2016, *MNRAS*, **458**, 3942
- Vogt, S. S., *et al.* 1994, in *Proc. SPIE Instrumentation in Astronomy VIII*, David L. Crawford; Eric R. Craine; Eds., Volume 2198, p. 362, edited by D. L. Crawford & E. R. Craine, vol. 2198 of *Presented at the Society of Photo-Optical Instrumentation Engineers (SPIE) Conference*, 362
- Wasson, J. T. & Kallemeyn, G. W. 1988, *Philosophical Transactions of the Royal Society of London Series A*, **325**, 535
- Wetzel, D. T., Hauri, E. H., Saal, A. E., & Rutherford, M. J. 2015, *Nature Geoscience*, **8**, 755
- Wilson, D. J., Gänsicke, B. T., Farihi, J., & Koester, D. 2016, *MNRAS*
- Wilson, D. J., Gänsicke, B. T., Koester, D., Toloza, O., Pala, A. F., Breedt, E., & Parsons, S. G. 2015, *MNRAS*, **451**, 3237
- Wyatt, M. C., Farihi, J., Pringle, J. E., & Bonsor, A. 2014, *MNRAS*, **439**, 3371
- Xu, S., Jura, M., Dufour, P., & Zuckerman, B. 2016, *ApJL*, **816**, L22
- Xu, S., Jura, M., Klein, B., Koester, D., & Zuckerman, B. 2013, *ApJ*, **766**, 132
- Xu, S., Jura, M., Koester, D., Klein, B., & Zuckerman, B. 2014, *ApJ*, **783**, 79

- Zhou, G., *et al.* 2016, *ArXiv e-prints*  
Zuckerman, B., Koester, D., Dufour, P., Melis, C., Klein, B., &  
Jura, M. 2011, *ApJ*, **739**, 101  
Zuckerman, B., Koester, D., Melis, C., Hansen, B. M., & Jura,  
M. 2007, *ApJ*, **671**, 872

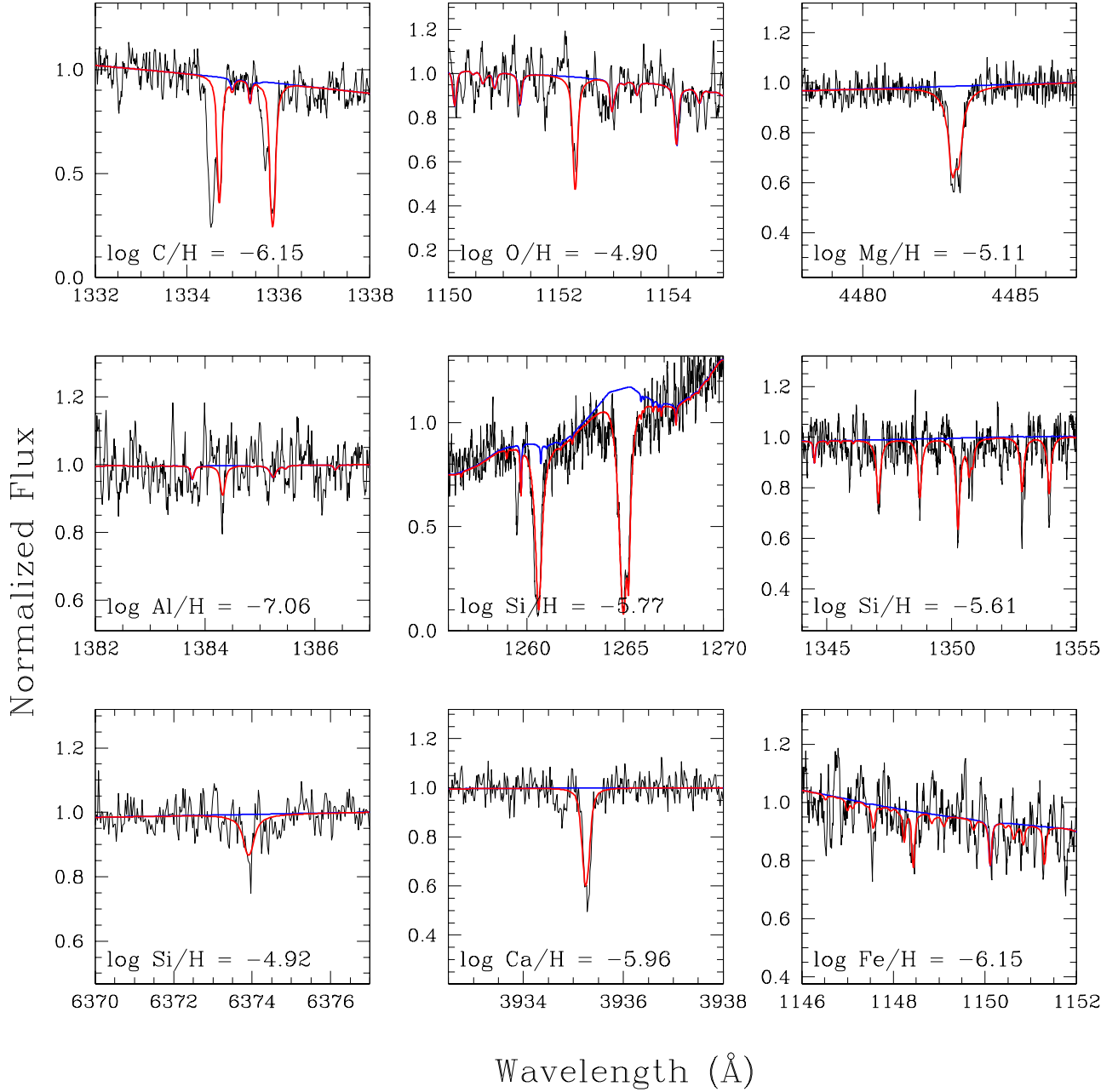


**Figure 1.** Elements identified in the *HST*/COS and Keck/HIRES spectra of SDSS J1043+0855. The black noisy curve is the data, smooth red curves are model fits, and blue curves with the element of interest removed show which line or lines are being considered. Lines not included in the fit in the C panel are from interstellar carbon (see Section 3). The multiple panels for Si demonstrate the disagreement between optical and ultraviolet abundances; see discussion in Section 3. All wavelengths are in vacuum and presented in the heliocentric reference frame. Measured abundances for the element of interest are indicated relative to H by number in each panel.



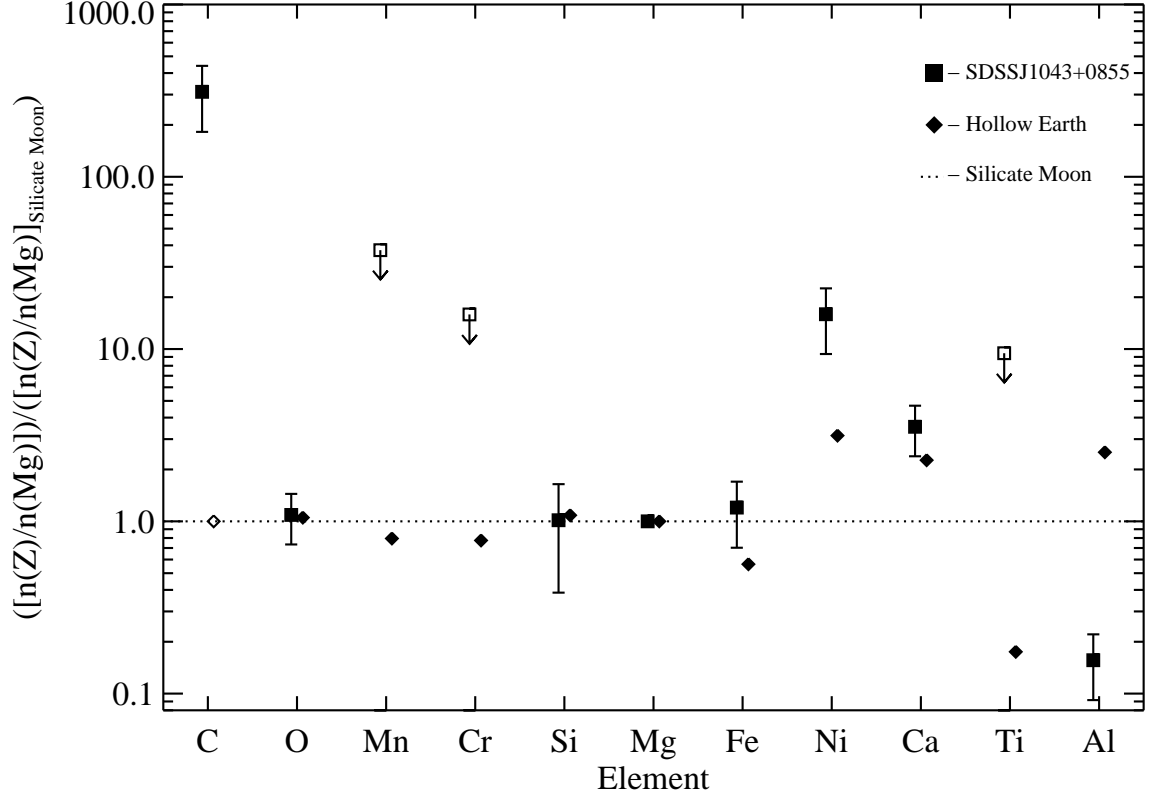


**Figure 2.** Abundances relative to Mg as compared to the silicate Moon (see Table 1); elements have increasing condensation temperature (for physical and chemical conditions within the Solar nebula) to the right. The square data points are measurements and upper limits for SDSS J1043+0855 from Table 1, uncertainties are  $\approx 50\%$  less than what would be expected by simple propagation of errors as discussed in Klein *et al.* (2010). The diamond data points are for a model where the core and lower mantle of the Earth are removed as described in Section 4. The dotted line is what would be expected if abundances relative to Mg exactly like the silicate Moon are realized. C measurements for the silicate Moon and the crust and mantle of the Earth are discussed in more detail in Section 4 and Table 1.

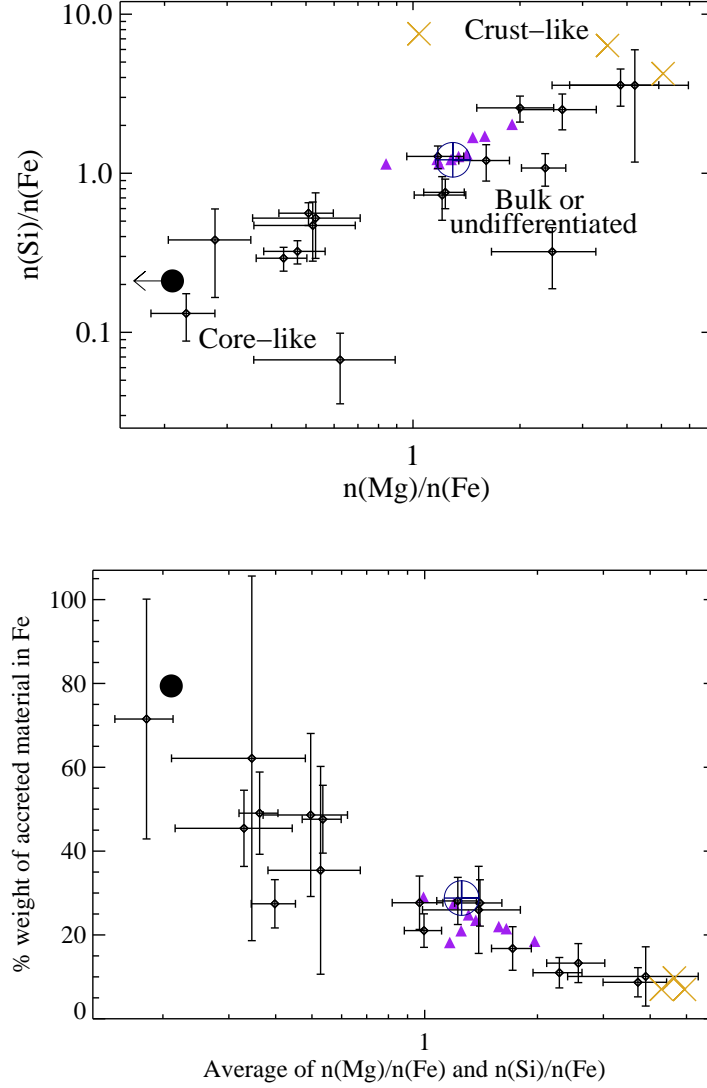


**Figure 3.** A trend when comparing accreted Si/Fe vs Mg/Fe abundance ratios (top panel) is suggestive of whether material accreted by white dwarfs originates from the inner or outer regions of a rocky body. Those objects with high relative levels of Fe lie in the region of the plot marked as “Core-like” as they are reminiscent of the Fe-dominated interior of differentiated rocky bodies. Those objects with low relative levels of Fe lie in the region marked as “Crust-like” as they appear significantly devoid of Fe as one might expect if the outer layers of a differentiated body were stripped and then accreted by the host white dwarf star. The bottom panel confirms the Fe-rich or Fe-poor nature of objects in these two regions. The large, gold-colored “X” points that lie in the “Crust-like” region mark the silicate Moon, bulk oceanic crust of the Earth, and bulk continental crust of the Earth. The silicate Moon has  $\text{Mg}/\text{Fe} \approx \text{Si}/\text{Fe} \approx 5$  and Fe mass fraction of  $\approx 10\%$  while the bulk continental crust of Earth has  $\text{Mg}/\text{Fe} \approx 1$ ,  $\text{Si}/\text{Fe} \approx 8$ , and Fe mass fraction of  $\approx 7\%$ . Small, filled purple triangle data points present chondrite data and are meant to represent extremely primitive rocky objects in the Solar system. The large, blue circle with a blue plus inside it near  $\text{Mg}/\text{Fe} \approx \text{Si}/\text{Fe} \approx 1.3$  is the Bulk Earth. The large, black filled circle is for the core of Earth which is based on extrapolations from chondrite data and assumes no Mg is in the core (Allègre *et al.* 1995); the Earth core value for Mg/Fe is set to Si/Fe for plotting purposes. White dwarf data come from Dufour *et al.* (2010, 2012), Zuckerman *et al.* (2011), Gänsicke *et al.* (2012), Farihi *et al.* (2013), Xu *et al.* (2013, 2014, 2016), Wilson *et al.* (2015), Raddi *et al.* (2015), and Farihi *et al.* (2016). Metal abundance ratio errors for white dwarf measurements are adjusted similar to those for SDSS J1043+0855 like in Figure 2. Percent weight of Fe errors are as propagated directly from the Fe abundance measurement error in the atmosphere of each white dwarf star. Bulk Earth and Earth core data are from Allègre *et al.* (1995), chondrite data from Wasson & Kallemeyn (1988), silicate Moon data from Lodders & Fegley (2011), and bulk oceanic and continental crust data from Anderson (1989).

**Table 1.** SDSS J1043+0855 Metal Pollution

$Z$	$\log[n(Z)/n(\text{H})]_{\text{measured}}$	$\log(\tau_{\text{diff}}/\text{years})^{\text{a}}$	$[n(Z)/n(\text{Mg})]_{\text{accreted}}^{\text{b}}$	$[n(Z)/n(\text{Mg})]_{\text{Silicate Moon}}^{\text{c}}$	$\dot{M}_{\text{acc}}/(10^7 \text{ g s}^{-1})^{\text{d}}$	% wt. <sup>e</sup>
C	$-6.15 \pm 0.30$	$-2.32$	0.13	0.0004	0.15	1.2
O	$-4.90 \pm 0.20$	$-2.48$	3.3	3.1	5.3	41
Mg	$-5.11 \pm 0.20$	$-2.16$	1.0	1.0	2.4	18
Al	$-7.06 \pm 0.30$	$-2.23$	0.013	0.084	0.035	0.27
Si	$-5.33 \pm 0.50$	$-2.31$	0.84	0.84	2.3	18
P	$-7.40 \pm 0.30$	$-2.41$	0.0091	0.00006	0.028	0.22
S	$-6.36 \pm 0.40^{\text{f}}$	$-2.54$	0.13	—	0.43	3.3
Ca	$-5.96 \pm 0.20$	$-2.36$	0.22	0.064	0.90	6.9
Sc	$< -7.5$	$-2.41$	$< 0.0072$	0.00003	$< 0.032$	$< 0.25$
Ti	$< -7.0$	$-2.44$	$< 0.024$	0.0025	$< 0.11$	$< 0.89$
V	$< -7.5$	$-2.47$	$< 0.0082$	0.0001	$< 0.042$	$< 0.32$
Cr	$< -6.5$	$-2.47$	$< 0.083$	0.0052	$< 0.43$	$< 3.3$
Mn	$< -6.5$	$-2.52$	$< 0.094$	0.0025	$< 0.52$	$< 3.9$
Fe	$-6.15 \pm 0.30$	$-2.58$	0.23	0.20	1.3	10
Ni	$-7.38 \pm 0.30$	$-2.56$	0.013	0.0008	0.078	0.60

<sup>a</sup>Diffusion constants, see [Koester \(2009\)](#) for discussion of what these values mean and Section 4 for where these values come from for the analysis presented herein.

<sup>b</sup>Parent body abundances relative to Mg; see Section 4 and Figure 2.

<sup>c</sup>Silicate Moon data from Table 4.7 of [Lodders & Fegley \(2011\)](#) with the exception of data for C which comes from [Wetzel et al. \(2015\)](#). See also Figure 2 and discussion in Section 4 for C.

<sup>d</sup> $\dot{M}_{\text{acc}}(Z) = M_{\text{env}}(Z)/\tau_{\text{diff}}(Z)$  where  $M_{\text{env}}(Z)$  is the mass of element  $Z$  in the hydrogen-dominated envelope of SDSS J1043+0855 assuming it has a mass of  $2.82 \times 10^{16} \text{ g}$  (see Section 4).

<sup>e</sup>Mass fraction of each element in percent weight as deduced from the relative contribution to the total  $\dot{M}_{\text{acc}}$ .

<sup>f</sup>Sulfur is tentatively detected and the suggested abundance can be taken as a firm upper limit.